ACS MATERIALS LETTERS

www.acsmaterialsletters.org

LETTER

Zinc-Assisted Microscale Granules Made of the SARS-CoV-2 Spike Protein Trigger Neutralizing, Antivirus Antibody Responses

Marianna T. P. Favaro,[▽] Patricia Alamo,[▽] Nerea Roher, Miguel Chillon, Jara Lascorz, Merce Márquez, José Luis Corchero, Rosa Mendoza, Carlos Martínez-Torró, Neus Ferrer-Miralles, Luis C. S. Ferreira, Ramón Mangues, Esther Vázquez, Eloi Parladé,* and Antonio Villaverde*

Cite This: *ACS Materials Lett.* 2024, 6, 954−962

Read Online

ACCESS | Metrics & More | Article Recommendations

ABSTRACT: **The development of new and more efficient vaccination approaches is a constant need, due to the pressure of historical and emerging infectious diseases and the limited efficacy and universality of the current vaccination technologies. Peptides and recombinant proteins have been explored for decades as subunit vaccines for bacterial and viral infections, presented either as soluble protein species or as virus-like assemblies. Recently, synthetic secretory protein-only microscale granules have been developed as dynamic depots for sustained protein release. They are based on the reversible coordination between ionic Zn and histidine residues, which promotes a fast formation of granular particles in vitro out of soluble protein and a slow release of such building block protein in vivo through the physiological chelation of the metal. Such an endocrine-like platform represents a new drug delivery system fully validated in oncology by which soluble and functional protein drugs are progressively released from the granules and made available for antitumor activities upon subcutaneous administration. By exploring such an approach for immunization here, microparticles made of a recombinant form of the receptor binding domain (RBD) of SARS-CoV-2 were tested as an antigen delivery system for induction of antibody responses against the virus upon administration of the material in the absence of added adjuvants. Also, the comparison between protein materials produced in bacterial, mammalian, or insect cell factories has demonstrated a moderate impact of protein glycosylation on the final immunological performance of the system. Therefore, we propose the consideration of synthetic protein secretory granules as a new sustainable immunization platform based on fully manageable, self-organized, and self-formulated immunogens, aimed at reducing the dosage, costs, and complexity of vaccination regimens.**

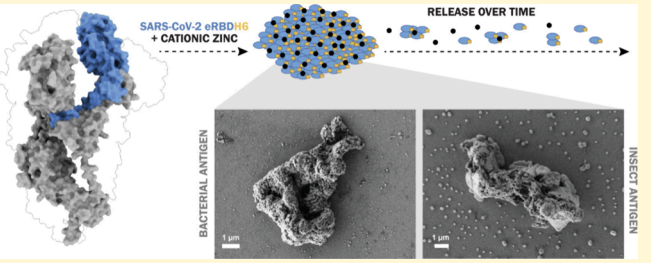

The emergence of infectious diseases is pushing toward the sustainable development of novel materials, instruments, and approaches for proper prophylaxis and therapies.[1,2] Because of the lack of generically usable antiviral drugs, efficient immunization against viral infections is particularly desired but not reachable through one universal approach. In contrast to the classical inactivation or attenuation of whole pathogens, largely used for smallpox, poliomyelitis, rabies, and other historical human or veterinary diseases,[3] genetic vaccines (based on expressible DNA or RNA) have emerged, pushed by the COVID-19 pandemics, as promising and fast-adapting tools for immunization.[4−6] Amid both types of technologies, protein-based subunit vaccines (including virus-like particles (VLPs),[7,8]) have been developed, tested, and adapted for decades.[9] They have mostly used immunodominant antigens from the target pathogen obtained in cell factories through scalable, cost-effective recombinant DNA procedures. Even though some prototypes have reached the market,[10] they have generally resulted in disappointing levels of immune activation and in limited effectiveness, that require repeated administrations and incorporation of adjuvants, resulting in high economic costs and logistic complexity.[11,12] Among other reasons, the failure in selecting or presenting the antigens in an appropriate way might be the

Received: December 23, 2023
Revised: February 7, 2024
Accepted: February 7, 2024
Published: February 14, 2024

https://doi.org/10.1021/acsmaterialslett.3c01643
ACS Materials Lett. 2024, 6, 954−962

cause for moderate immune responses.[12−14] In previous studies, we have developed Zn-supported protein-releasing microscale granular materials[15] that, upon subcutaneous injection, act as intriguing drug-delivery systems.[16] These protein granules are formed by pure protein preparations in which the individual polypeptide chains are clustered together into insoluble aggregates by the fast coordination between histidine residues of soluble proteins and divalent cations.[17,18] In the absence of local or systemic toxicities,[19] the resulting micrometer-scale particles disassemble, through a self-disintegrating process in vivo, into functional building block polypeptides, during prolonged time periods.[15] Both the structure and mechanics of the synthetic granular materials are similar to those of natural protein depots of protein/peptide hormones in the mammalian endocrine system,[20−24] Therefore, the observed protein leakage from the artificial materials, based on Zn chelation[25] can be considered a secretion-like event within an endocrine-like process. While these emerging manufactured materials have been fully validated in oncology,[25,26] so far, their applicability to other clinical areas has been neglected. Then, we wondered if the unique presentation of a pathogen-derived antigen in such a formulation (protein releasing microgranules) might be appropriate for immune activation and if such an approach might reduce the number of administrations and, therefore, the costs and complexity of the vaccination protocols. In this context, we have recently approached the comparative fabrication of secretory granules out from a single model protein (the extended receptor binding domain -eRBD- from the SARS-CoV-2 spike protein) obtained in three different cell factories, namely bacteria, insect cells and mammalian cells.[27] These materials have been preliminarily explored here as immunogens in mice and the quality of the elicited immune responses have been analyzed through the induction of neutralizing antibodies over infectious SARS-CoV-2 virus particles.

The eRBD protein was designed to comprise the extended sequence of RBD from SARS-CoV-2 (Figure 1A), being successfully produced as described[27] in three different cell factories, namely, bacteria (*E. coli*), insect cells (SF9), and mammalian cells (EXPI), without (from bacteria) or with different glycosylation patterns, respectively. The presence and type of glycosylation was the only clear structural difference observed between these protein versions, since other physicochemical properties were essentially indistinguishable among them.[27] Proteins obtained from these different expression systems were evaluated here as soluble antigens or protein-leaking dynamic depots (Figure 1B). These depots organize as microscale granular protein clusters generated in vitro by the addition of a molar excess of cationic Zn.[28] With a size ranging from ∼3 to 70 μm and an average of 20.3 ± 17.0 μm, these materials release the forming building blocks upon in vivo administration, mimicking the behavior of the hormone granular depots from the human endocrine system.

Soluble versions of these antigens were subcutaneously administered in mice according to conventional immunization protocols, namely, in two doses of 100 μg each (at days 0 and 21), formulated with the conventional adjuvant Addavax, which is a MF59 mimetic.[29] Other groups of animals were equally immunized with 300 μg of the granular version of these antigens, always following the vaccination regimen described in Figure 1C.

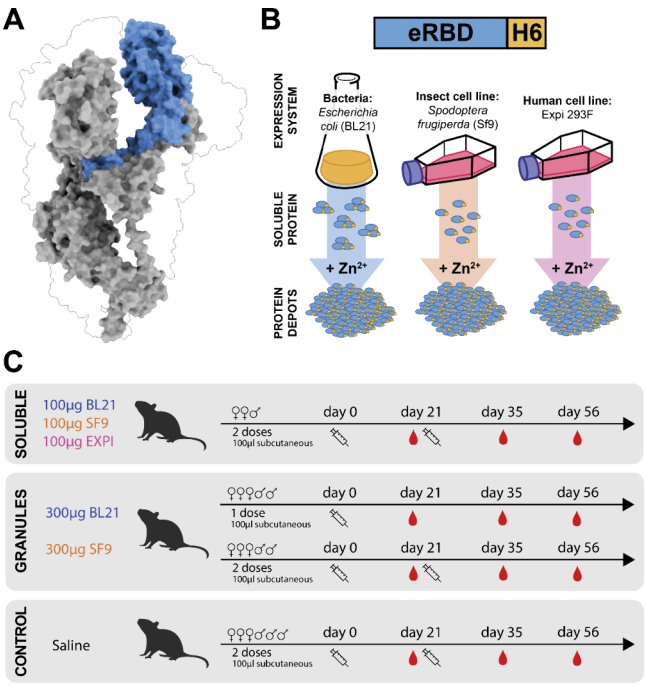

Figure 1. Conceptualization of eRBD production and immunization regimens. (A) Scheme of the spike protein trimer of SARS-CoV-2, highlighting a subunit in gray and the eRBD (residues 300−545, GenBank: QHD43416.1) region used in the present study in blue. (B) Representation of the approaches used for recombinant protein expression and further formation of granules that constitute protein depots. (C) Schematic representation of the immunization regimes.

As observed (Figure 2A), all recombinant protein versions induced detectable anti-SARS-CoV-2 IgG antibodies when administered as soluble adjuvanted antigens, showing a positive time evolution. Especially regarding the BL21 and SF9 products, specific antibodies were not detected at 21 days. Although with nonsignificant differences at the end point (56 days) due to high variance, the IgG responses elicited by mammalian cells were strong and consistent since the first evaluation at 21 days. In a more robust trend, antigens derived from insect cells took longer to trigger specific antibodies but ended up providing the highest anti-SARS-CoV-2 IgG levels. The virus neutralizing responses induced by all the tested antigen types were also comparable among candidates, with values slightly higher, again, in the case of the product from insect cells (Figure 2B). At the concentration tested (100 μg of soluble antigen), insect and mammalian antigens induced a statistically relevant neutralizing response against viral particles in viral neutralization assays. Despite showing no statistical differences with other tested versions, the bacterial antigen has an observable neutralizing effect compared with the control group administered with saline. The animals' weight, a common key parameter used in toxicity determinations,[30] was monitored for the duration of the experiment, with male and female data plotted separately since their initial values differed and since they progressed slightly different. Weight of immunized animals showed steady increases within the expected range without significant differences in comparison with the saline group (Figure 2C). The regular body weight progression was then fully consistent with lack of toxicity of the administered proteins. Altogether, the data depicted above demonstrate that immunization with Zn-assisted granular

https://doi.org/10.1021/acsmaterialslett.3c01643
ACS Materials Lett. 2024, 6, 954−962

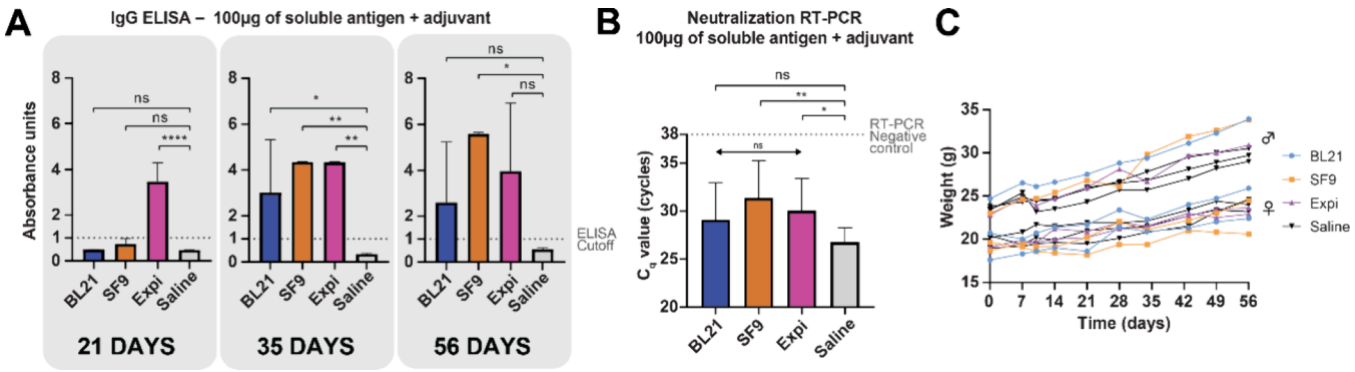

Figure 2. Immunization with the soluble versions of eRBD. (A) Anti-SARS-CoV-2 IgG antibody levels determined at various times upon antigen administration (which occurred subcutaneously at days 0 and 21). (B) Neutralization capacity of the animal sera (collected at day 56) against infectious SARS-CoV-2 particles. Vaccine doses were administered subcutaneously on days 0 and 21. (C) Weight followup of animals immunized with soluble antigens.

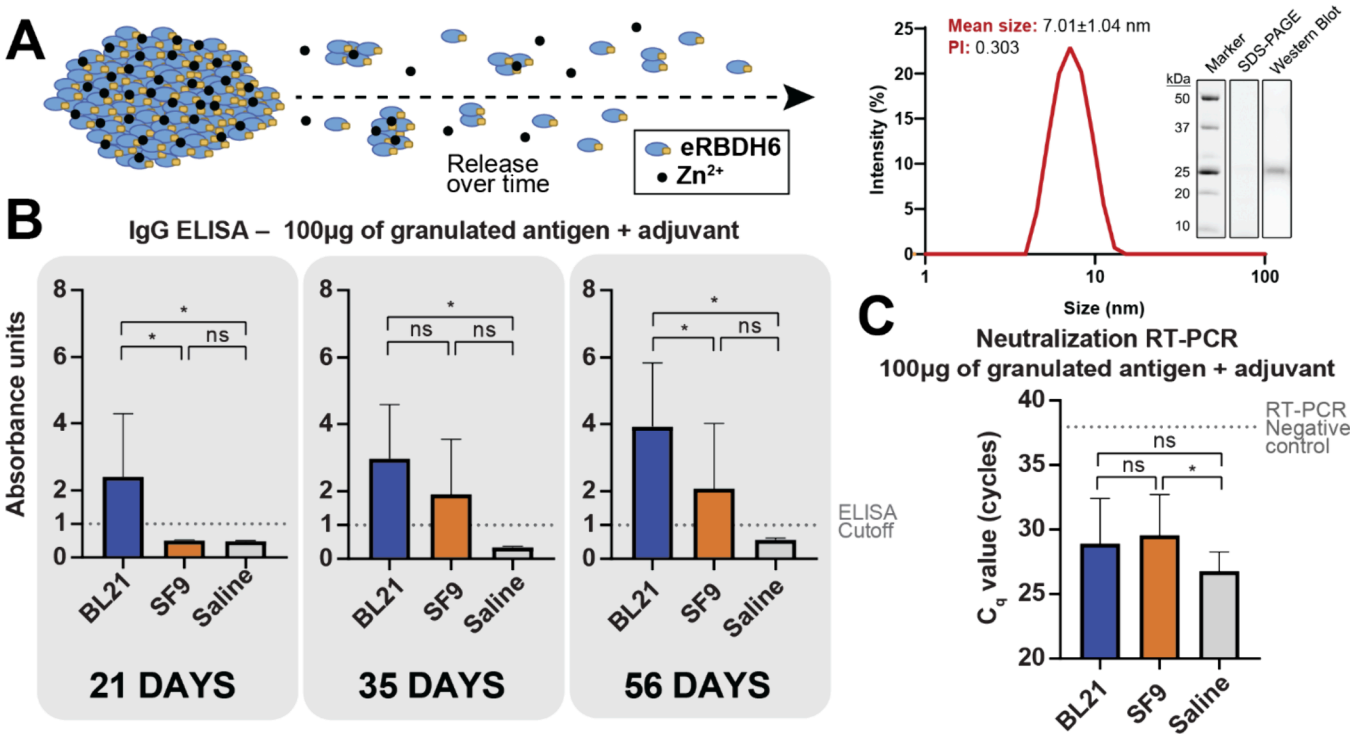

Figure 3. Immunization with the microparticle versions (granules) of eRBD combined to adjuvant. (A) (Left panel) Scheme of the performance of secretory microscale granules and of their protein-release dynamics. (Right panel) Size and molecular weight of the protein leaked in vitro from BL21 protein granules after 24 h of incubation at 37 °C in PBS. The inset features SDS-PAGE and Western blot images of the released fraction, confirming full protein integrity. (B) Anti-SARS-CoV-2 antibody levels determined at various times upon antigen administration. Vaccine doses were administered subcutaneously at days 0 and 21. (C) Neutralization capacity of the animal sera (collected at day 56) over infectious SARS-CoV-2 particles.

depots preserves immunological features of the SARS CoV-2 RBD protein with minor influence of the cell factory used for production of the recombinant antigen.

Then, the preliminary set of neutralization data was also suggestive that the glycosylation pattern was moderately relevant to the quality of the triggered antibody response, while the quantity of induced antibodies might be affected by the type of glycosylation. At this point, we decided to explore how these antigens might behave once they are formulated as secretory protein granules. These structures are capable of gradually releasing building block proteins in monomeric or oligomeric forms (Figure 3A) in its full-length intact form (28.6 kDa), as confirmed here for the bacterial protein (Figure 3A). This was indicative of the competent proteolytic stability of the polypeptides when clustered in microscale granules.

In the context of the prolonged protein release associated with this new protein material, it has been recently demonstrated that a slow and controlled release of antigens is associated with improved immunological responses,[31] a fact that might confer appealing properties to protein-leaking depots. Since the soluble protein obtained in mammalian cells did not result in stable aggregates upon exposure to cationic Zn,[27] the study of secretory granules was limited to bacterial and insect cell products. In this regard, data presented in Figure 2 suggest that the RBD version produced by Expi cells has no clear advantages, in comparison with the SF9

https://doi.org/10.1021/acsmaterialslett.3c01643
ACS Materials Lett. 2024, 6, 954−962

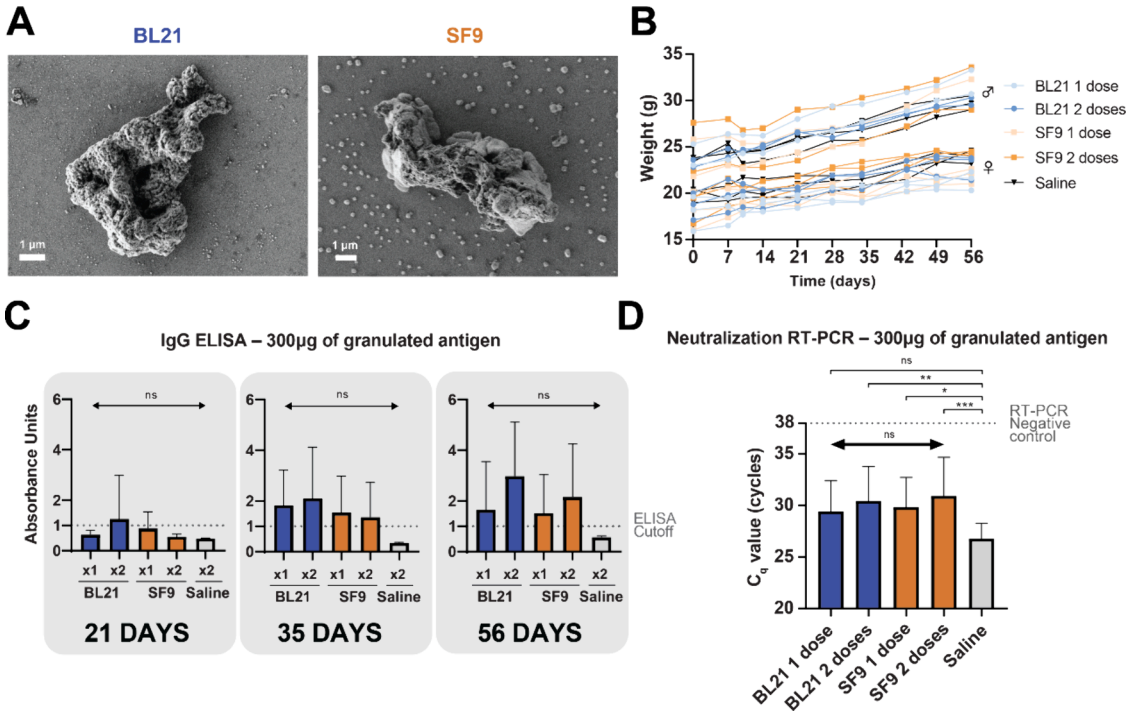

Figure 4. Immunization with microparticle versions (granules) of eRBD. (A) Representative FESEM images of secretory granules formed by eRBD from either BL21 or SF9. (B) Weight followup of immunized mice. (C) Anti-SARS-CoV-2 antibody responses determined at different times upon antigen administration, which was done subcutaneously either at day 0 (one dose, ×1) or at day 0 and at day 21 (two doses, ×2). (D) Neutralization capacity of the animal sera (collected at day 56) against infectious SARS-CoV-2 particles.

counterpart, in terms of neither IgG levels nor neutralization capacity. Therefore, the study, as limited to two alternative products, would be highly valuable. These two types of depots were combined with Addavax and administered following the vaccination regimen indicated in Figure 1C (two doses, at days 0 and 21, respectively). Formulated in such a way, and in the presence of adjuvant, both antigens triggered antigen-specific serum (IgG) antibody responses (Figure 3B) and neutralizing antibody responses over infectious viral particles (Figure 3C). However, the effectiveness of the triggered responses could only be evidenced statistically in terms of antibody production for the BL21-derived antigen and in neutralization for the SF9-derived antigen. Despite this, no significant differences in the viral neutralization effects were observed between antigen types, suggesting that potency in terms of virus neutralization activity was present, irrespective of the cell factory used for protein production (Figures 3B and 3C).

In a step further, we decided to explore if the administration of the materials per se, without the addition of adjuvant, would be sufficient for proper immune stimulation. For that, the protein dose was adjusted to the percentage of protein (~30%) that is released from the granules (and therefore bioavailable) during the first days.[16] We first confirmed the morphology and stability of secretory microgranules by FESEM (Figure 4A). The followup of mice immunized with these materials revealed that the administration of secretory granules had no relevant impact on body weight (Figure 4B), again indicative of the absence of acute toxicities, as discussed above. As observed, without any adjuvant, both one single and double shots of granules resulted in relevant serum antigen-specific IgG responses (Figure 4C), while the administration of a second dose seems to be supportive of a better induction of antiviral neutralizing antibodies (Figure 4D). Overall, the secretory microgranules were able to trigger antibody responses and neutralization potencies comparable to those detected by a conventional immunization approach with an adjuvanted soluble antigen (Figure 2). Interestingly, both protein products rendered similar responses, irrespective of the cell factory used for production, and the administration of a second protein bolus slightly increased the reached antibody titers (despite not in a significant manner, Figure 4C).

Synthetic microscale secretory granules, made of his-tagged recombinant proteins, have been recently developed as novel protein-release platforms.[15,32] Being dynamic protein-releasing depots supported by metal-protein coordination, they mimic the architecture and functionalities of the secretory granules of peptide hormones from the mammalian endocrine system.[21−23] The artificial material versions are fabricated in vitro by simple procedures out of pure soluble, his-tagged recombinant proteins, by the coordination of the imidazole rings from histidine residues with ionic Zn or other divalent cations.[17,28] This property generates reversible links between histidine residues from different polypeptidic chains and, thus, a cross-linking effect.[33] The mechanical stability of secretory granules is sustained by their amyloid content;[15] they are, in fact, considered members of the category of functional, nontoxic amyloids abounding in Nature.[34−38] This specific type of aggregate is reversible,[39−43,] and this feature ensures the bioavailability of functional proteins to support the cellular or organic needs.[44,45] Both in vitro and upon subcutaneous administration, the granules disassemble into the forming building block polypeptides or into oligomeric forms of them,[15,25,46] that reach the bloodstream available for the intended protein functionality.[15,47] Previous studies with synthetic granules formed by cytotoxic proteins, growth factors, or highly specific cell surface peptidic ligands,[15,48]

https://doi.org/10.1021/acsmaterialslett.3c01643
ACS Materials Lett. 2024, 6, 954−962

whose functions are highly conformation-dependent, demonstrated that the released protein keeps, as in the natural counterparts, the native conformation. Also, a recombinant β-galactosidase clustered by ionic Zn, is functional within the artificial granules, and it is able to perform its catalytic activities.[49]

In the context of these properties regarding the conservation of the protein conformation, we have proved here that secretory granules formed by SARS-CoV-2 eRBD stimulate a humoral neutralizing response upon in vivo administration in the absence of adjuvant (Figure 3). The potency of this response is comparable to that triggered when administering the mere building blocks (the soluble eRBD species) in a conventional two-dose adjuvation (Figure 2). It is noteworthy that the adjuvant used, Addavax, is a squalene-based oil-in-water emulsion that was previously reported to boost immune responses against vaccine formulations, without affecting antigen conformation in protein nanoparticles.[50]

The protein leakage from the microscale protein granules is mediated by a dilution of the clustering Zn cations from the complexes, which results in the progressive disassembling of the his-tagged monomers and their release from the depot core. In fact, during the formation of amyloid protein nuclei, there is a recruit of soluble building block versions to reach a steady-state equilibrium between insoluble and soluble forms.[24] Then, the depots, upon dilution, are also able to release the forming proteins in a functional, properly folded version,[24] which is corroborated by the fact that eRBD released from granules is capable of eliciting neutralizing antibodies that recognize the native protein in the viral particle. The whole set of such events define a slow protein-release platform that, in vivo, is the source of soluble protein for at least 1 week or more.[25] When using antigens as building blocks, the administration of the granules results in a prolonged exposure of the immune system to them in a comparable way in which an antigen from a replicating microbe is seen during a natural acute infection.[51] Since the success of vaccination is at least partially observed because of a prolonged exposure to antigens,[31] we speculated that secretory granules might be good immunostimulatory agents. In fact, the slow release of eRDB from Zn-assisted depots had been already demonstrated in vitro,[27] as well as their lack of toxicity.[19] Being the amount of Zn in the granules (∼5 mg per dose) much lower than the recommended daily intake for humans (with an upper limit of ∼40 mg/day)[17] and much far below the range of the metal in the human body (2−4 g),[52] the presence of the metal should not be a matter of concern. It must be noted that, in addition, other divalent cations such as Ca, which is much more abundant than Zn in the mammalian bodies (estimated to be higher than 1000 g), have been proven to be also suited for the construction of secretory granules.[15,25] Importantly, Zn shows itself immunomodulating properties, and then, it is a supporter of the antigen-specific immune response.[53] Therefore, the use of this particular metal for the fabrication of the granules and its presence in the administered material, even at very low levels, might represent an added value regarding the immunogenic potential of the whole platform. Not needing external adjuvant, the secretory granules developed here are then self-organized, self-formulated antigen delivery platforms for a time-prolonged immune stimulation.

This is of course a proof of concept that needs further development, and accumulative testing of the self-disintegrating material under different experimental setups is largely required. However, the fact that the administration of eRBD depots (followed by the natural prolonged dosage during depot disintegration), in the absence of externally added adjuvant, triggers efficient neutralizing responses (Figure 3B) might allow one to approach the dilemma about the number of necessary shoots in vaccination.[54−57] Also, the hope of skipping the adjuvant in the final formulation, a possibility that is currently being tested through very different alternative approaches,[58−60] is appealing from the viewpoint of safety and economy. Furthermore, previous studies about the stability of cation-induced protein aggregation attribute a higher structural stability, under different physicochemical conditions, to the clustered protein versions, compared to soluble ones.[16,61] This means that any storage conditions intended for conventional protein drugs should be suited for adaptation to granular depots, including 4 °C, freezing, and lyophilization. This fact allows envisaging smooth distribution routes for potential future vaccine preparations based on the concepts described here.

In the context of approaching a circular and sustainable economy and because of the increasing global demands of human and veterinary immunization programs, unfeasible in specific geography areas, exploring, developing, and implementing adjuvant-free vaccines based on a single depot shoot might represent a paradigmatic shift.

We have demonstrated here, by using a SARS-CoV-2 protein (RBD) as a model, how an emerging endocrine-like antigen-releasing system induces an antibody-based antiviral neutralizing response. This is reachable upon a single, adjuvant-free subcutaneous administration of dynamic microgranular depots that results in a time-prolonged dosage and consequent sustained antigenic exposure to the immune system. Although deserving further investigation regarding the transversal character of the system, the presented data open a door to a significant reduction of costs, chemicals, and complexity in the administration of protein-based vaccines through self-organized, self-formulated, protein-releasing dynamic depots.

EXPERIMENTAL SECTION

Protein Synthesis and Granule Preparation. eRBD is an elongated form of the receptor binding domain (RBD) from the SARS-CoV-2 virus. For production in *Escherichia coli*, the gene was incorporated into a pET22b plasmid vector and subsequently expressed in *E. coli* BL21 DE3 cells (Novagen-Merck, Darmstadt, Germany) with a hexahistidine tag in the C-terminus. The procedures for protein production in the form of inclusion bodies and the further refolding processes to obtain soluble protein were previously described elsewhere.[27] In insect cells, the production of eRBD was carried out by transiently transfecting SF9 cells with plasmid pIZT/V5-His encoding the gene sequence with the gp67 secretion signal peptide in the N-terminus. This was followed by protein purification from the clarified supernatant of SF9 culture by combining affinity chromatography and subsequent size exclusion chromatography, as previously described.[28] In mammalian cells, eRBD was produced by transfection and transient gene expression in the mammalian cell line Expi293 cells following the manufacturer's instructions and purified from the supernatant using a combination of affinity capture, followed by two polishing steps based on ion exchange chromatography, as described previously.[28]

https://doi.org/10.1021/acsmaterialslett.3c01643
ACS Materials Lett. 2024, 6, 954−962

The formation of protein-leaking microparticles, which represent an insoluble material, was accomplished from the obtained soluble protein versions via a modified version of a previously established method.[28] In summary, the secretory granules were generated by mixing the protein with a molar excess of ionic zinc (Zn^{2+}), relative to the number of histidine residues present in the H6 tag. Specifically, the soluble protein was combined with $ZnCl_2$ in a molar ratio of 1:300 (protein:cation), within a potassium−sodium phosphate-buffered saline solution maintaining pH 7.4 (physiological pH). Following a 10 min incubation period for the reaction to take place, the samples were subjected to centrifugation at 15 000*g* for 15 min to segregate the insoluble microgranules from the remaining unreacted soluble protein present in the supernatant.

Western Blot and Protein Size Measurement. To assess the integrity of the polypeptides released from microparticles, these materials were first resuspended in PBS and incubated for 24 h at 37 °C. Samples from the soluble fraction were then analyzed by SDS-PAGE and further Western blot tests. SDS-PAGE was performed by using TGX Stain-Free FastCast acrylamide 12% (Bio-Rad, Hercules, CA, USA), and protein bands were visualized with a ChemiDoc Touch Imaging System (Bio-Rad, Hercules, CA, USA). To reveal immunoreactive bands in Western blots, an anti-His mouse monoclonal antibody (from GeneScript, Piscataway, NJ, USA, Ref. No. A00186-100) was used as the primary antibody. The determination of the molecular hydrodynamic size was carried out via dynamic light scattering (DLS) at 633 nm, in a Zetasizer Nano ZS (Malvern Instruments, Malvern, U.K.), operating at a controlled temperature of 25 °C. For that, 60 μL of undiluted supernatants were measured in triplicate in a low-volume cuvette. Data were processed in the ZS XPLORER software (version 2.0.1.1).

Microscopy. High-resolution electron microscopy images of the eRBD microparticles were captured by using a field-emission scanning electron microscopy (FESEM) instrument, specifically the Zeiss Merlin (Oberkochen, Germany), operating at 1 kV and equipped with a high-resolution secondary electron detector.

In Vivo Experiments. Experiments were conducted following European Council directives and were approved by the Mouse Ethics Committee at Hospital de la Santa Creu i Sant Pau (Procedure No. 9721). Male and female BALB/c mice, aged 6−8 weeks, and weighing between 16 and 27 g, were obtained from Charles River (L'Arbresle, France) and were housed in a sterile environment with bedding, water, and γ-ray-sterilized food ad libitum. The administration regimen included 1 or 2 repeated doses of different amounts of microgranules of eRBD (300 or 100 μg), 2 repeated doses of 100 μg of soluble eRBD protein, or PBS in the control groups. Mice were randomly allocated in each group with doses administered on days 0 and 21. The administration was performed subcutaneously in the mouse lumbar region using a pellet of protein antigen granules suspended in 100 μL of PBS buffer. However, groups injected with 100 μg of either microgranules or soluble protein were resuspended in 50 μL of Addavax and 50 μL of PBS buffer. Mice were weighed 3 times a week to monitor for any weight loss. Animals in control groups were injected with 100 μL of a saline solution (sterile 0.9% NaCl, B. Braun, Spain).

Humoral response. On days 21, 35, and 56 after the initial injection, blood samples were collected from the mice to measure the humoral response to the protein antigen. The collected sera were analyzed for antibody levels using the Recombivirus Mouse Anti SARS-CoV-2 (COVID) Spike 1 RBD IgG ELISA Kit (RV-405420 Alpha Diagnostics, San Antonio, TX, USA), following the manufactureŕs instructions.

In Vitro Neutralization Assay. Briefly, 7.5 μL of each animal serum were incubated (Biosafety Level 3) at room temperature in a volume of 50 μL with 20 or 50 plaque-forming units of SARS-CoV2 (Strain: hCoV19/Spain/SP-VHIR.02, D614G(S)). Five independent replicates were analyzed per serum. After 1 h, the preincubated serum was resuspended in a final volume of 300 μ L (DMEM + 10% heat-inactivated serum) and added to 24-well plates of VeroE6 cells (70%−80% confluency). Six hours later, cells were washed three times with fresh media to remove remaining SARS-CoV-2 particles. At 24 or at 48 h post-infection, 100 μL were taken and centrifuged for 1 min at 10 000*g*, and 75 μL of the supernatant were transferred to a new tube and inactivated with RNA Shield in a 1:1 ratio (Zymo Research). The viral RNA was extracted using Quick-RNA viral kit (Zymo Research) following manufacturer's recommendations and further retrotranscribed using the Sensifast cDNA synthesis kit (Meridian). RT-qPCR against was performed using a Sensifast SYBR No-ROX kit (Meridian). Each sample was analyzed by qPCR per duplicate. Amplification conditions were as follows: (95 °C, 10 s + 60 °C, 1 min) × 40 cycles. (Ramp = 1.6 °C/s); primers, FW 5′- gaccccaaaatcagcgaaat-3′, RV 5′- tctggttactgccagttgaatctg, and probe 5′-FAM-accccgcat-tacgtttggtggacc-BHQ1−3′. Procedure No. HR632-21 was approved by the Biosafety Committee of the UAB. Results are expressed in Cq values or cycle quantification values that indicate the number of PCR cycles needed for the target nucleic acid to reach a detectable threshold. Hence, lower Cq values signify higher viral RNA concentrations, serving as a measure of the initial viral load.

Statistical Analysis. Data are presented as mean ± standard deviation. Statistical analyses were performed using GraphPad Prism version 8.0.2 (GraphPad Software, San Diego, CA, USA). Differences between groups were analyzed using a two-way ANOVA test, followed by Bonferroni's multiple comparisons test, and $p < 0.05$ was considered statistically significant.

AUTHOR INFORMATION

Corresponding Authors

Eloi Parladé − *Institut de Biotecnologia i de Biomedicina, Universitat Autònoma de Barcelona, 08193 Bellaterra, Spain; CIBER de Bioingeniería, Biomateriales y Nanomedicina (CIBER-BBN, ISCIII), Institut de Recerca Sant Pau, 08041 Barcelona, Spain;* orcid.org/0000-0001-5750-550X; Email: eloi.parlade@uab.cat

Antonio Villaverde − *Institut de Biotecnologia i de Biomedicina, Universitat Autònoma de Barcelona, 08193 Bellaterra, Spain; CIBER de Bioingeniería, Biomateriales y Nanomedicina (CIBER-BBN, ISCIII), Institut de Recerca Sant Pau, 08041 Barcelona, Spain; Departament de Genètica i de Microbiologia, Universitat Autònoma de Barcelona, 08193 Bellaterra, Spain;* orcid.org/0000-0002-2615-4521; Email: antoni.villaverde@uab.cat, antoni.Villaverde@uab.es, prof.a.villaverde@gmail.com

https://doi.org/10.1021/acsmaterialslett.3c01643
ACS Materials Lett. 2024, 6, 954−962

Authors

Marianna T. P. Favaro − *Institut de Biotecnologia i de Biomedicina, Universitat Autònoma de Barcelona, 08193 Bellaterra, Spain; Instituto de Ciências Biomédicas, Universidade de São Paulo, São Paulo 05508-000, Brazil*

Patricia Alamo − *Institut de Recerca Sant Pau, Barcelona, (IR Sant Pau), 08041 Barcelona, Spain; Josep Carreras Leukaemia Research Institute (IJC), 08916 Badalona, Spain; CIBER de Bioingeniería, Biomateriales y Nanomedicina (CIBER-BBN, ISCIII), Institut de Recerca Sant Pau, 08041 Barcelona, Spain*

Nerea Roher − *Institut de Biotecnologia i de Biomedicina, Universitat Autònoma de Barcelona, 08193 Bellaterra, Spain; CIBER de Bioingeniería, Biomateriales y Nanomedicina (CIBER-BBN, ISCIII), Institut de Recerca Sant Pau, 08041 Barcelona, Spain; Department of Cell Biology, Animal Physiology and Immunology, Universitat Autònoma de Barcelona, 08193 Bellaterra, Spain*

Miguel Chillon − *Department of Biochemistry and Molecular Biology, Institut de Neurociències (INc), Universitat Autònoma de Barcelona, 08193 Bellaterra, Spain; Vall d'Hebron Institut de Recerca (VHIR), 08035 Barcelona, Spain; Unitat Producció de Vectors (UPV), Universitat Autònoma de Barcelona, 08193 Bellaterra, Spain; Institució Catalana de Recerca i Estudis Avançats (ICREA), 08010 Barcelona, Spain*

Jara Lascorz − *Institut de Biotecnologia i de Biomedicina, Universitat Autònoma de Barcelona, 08193 Bellaterra, Spain; CIBER de Bioingeniería, Biomateriales y Nanomedicina (CIBER-BBN, ISCIII), Institut de Recerca Sant Pau, 08041 Barcelona, Spain*

Merce Márquez − *Institut de Biotecnologia i de Biomedicina, Universitat Autònoma de Barcelona, 08193 Bellaterra, Spain*

José Luis Corchero − *Institut de Biotecnologia i de Biomedicina, Universitat Autònoma de Barcelona, 08193 Bellaterra, Spain; CIBER de Bioingeniería, Biomateriales y Nanomedicina (CIBER-BBN, ISCIII), Institut de Recerca Sant Pau, 08041 Barcelona, Spain*

Rosa Mendoza − *Institut de Biotecnologia i de Biomedicina, Universitat Autònoma de Barcelona, 08193 Bellaterra, Spain; CIBER de Bioingeniería, Biomateriales y Nanomedicina (CIBER-BBN, ISCIII), Institut de Recerca Sant Pau, 08041 Barcelona, Spain*

Carlos Martínez-Torró − *Institut de Biotecnologia i de Biomedicina, Universitat Autònoma de Barcelona, 08193 Bellaterra, Spain; CIBER de Bioingeniería, Biomateriales y Nanomedicina (CIBER-BBN, ISCIII), Institut de Recerca Sant Pau, 08041 Barcelona, Spain*

Neus Ferrer-Miralles − *Institut de Biotecnologia i de Biomedicina, Universitat Autònoma de Barcelona, 08193 Bellaterra, Spain; CIBER de Bioingeniería, Biomateriales y Nanomedicina (CIBER-BBN, ISCIII), Institut de Recerca Sant Pau, 08041 Barcelona, Spain; Departament de Genètica i de Microbiologia, Universitat Autònoma de Barcelona, 08193 Bellaterra, Spain;* orcid.org/0000-0003-2981-3913

Luis C. S. Ferreira − *Instituto de Ciências Biomédicas, Universidade de São Paulo, São Paulo 05508-000, Brazil;* orcid.org/0000-0002-4883-1693

Ramón Mangues − *Institut de Recerca Sant Pau, Barcelona, (IR Sant Pau), 08041 Barcelona, Spain; Josep Carreras Leukaemia Research Institute (IJC), 08916 Badalona, Spain; CIBER de Bioingeniería, Biomateriales y Nanomedicina (CIBER-BBN, ISCIII), Institut de Recerca Sant Pau, 08041 Barcelona, Spain*

Esther Vázquez − *Institut de Biotecnologia i de Biomedicina, Universitat Autònoma de Barcelona, 08193 Bellaterra, Spain; CIBER de Bioingeniería, Biomateriales y Nanomedicina (CIBER-BBN, ISCIII), Institut de Recerca Sant Pau, 08041 Barcelona, Spain; Departament de Genètica i de Microbiologia, Universitat Autònoma de Barcelona, 08193 Bellaterra, Spain*

Complete contact information is available at: https://pubs.acs.org/10.1021/acsmaterialslett.3c01643

Author Contributions

[▽]M.T.P.F. and P.A. contributed equally to this work. The manuscript was written through contributions of all authors. All authors have given approval to the final version of the manuscript. C.M.-T., E.V., and A.V. are coinventors in a patent covering the use of artificial protein depots as immunogens. CRediT: **Marianna T. P. Favaro** investigation, methodology, writing-review & editing.

Funding

The authors appreciate the financial support received from AGAUR (2020PANDE00003 and 2021SGR00092 to A.V.), from CIBER-Consorcio Centro de Investigación Biomédica en Red- (CB06/01/0014), Instituto de Salud Carlos III, Ministerio de Ciencia e Innovación, through intramural projects (NANOSARS to E.P. and NANOREMOTE to E.V.). We also appreciate the support from AEI for the development of multimeric recombinant drugs (PID2019-105416RB-I00/AEI/10.13039/501100011033 and PDC2022-133858-I00 to E.V., PID2019-107298RB-C22 to N.F.-M., PID2020-116174RB-I00 to A.V. and PID2022-1368450 OB-10/AEI/10.13039/501100011033 to A.V. and E.V.). M.T.P.F. received a FAPESP fellowship (No. 2021/08528-0) and L.C.S.F. received a FAPESP research grant (No. 2020/05204-7). A.V. received an ICREA ACADEMIA award.

Notes

The authors declare the following competing financial interest(s): CMT, EV, and AV are co-inventors in a patent covering the use of artificial protein depots as immunogens.

■ ACKNOWLEDGMENTS

We are thankful to Luis Carlos Navas from Institut d'Investigacions Biomèdiques Sant Pau (IIB Sant Pau) for his technical support in in vivo experiments. Protein production was partially performed by the ICTS "NANBIOSIS", more specifically by the Protein Production Platform of CIBER in Bioengineering, Biomaterials & Nanomedicine (CIBER-BBN)/ IBB, at the UAB (http://www.nanbiosis.es/portfolio/u1-protein-production-platform-ppp/).

■ ABBREVIATIONS

ELISA, enzyme-linked immuno assay; FESEM, field-emission scanning electron microscopy; RBD, receptor-binding domain; SARS, severe acute respiratory syndrome; VLP, virus-like particle

■ REFERENCES

(1) Irvine, D. J.; Swartz, M. A.; Szeto, G. L. Engineering Synthetic Vaccines Using Cues from Natural Immunity. *Nat. Mater.* **2013**, *12*, 978.

(2) Roth, G. A.; Picece, V. C. T. M.; Ou, B. S.; Luo, W.; Pulendran, B.; Appel, E. A. Designing Spatial and Temporal Control of Vaccine Responses. *Nat. Rev. Mater.* **2022**, *7*, 174.
(3) Amanna, I. J.; Slifka, M. K. Wanted, Dead or Alive: New Viral Vaccines. *Antiviral Res.* **2009**, *84*, 119.
(4) Pushparajah, D.; Jimenez, S.; Wong, S.; Alattas, H.; Nafissi, N.; Slavcev, R. A. Advances in Gene-Based Vaccine Platforms to Address the COVID-19 Pandemic. *Adv. Drug Delivery Rev.* **2021**, *170*, 113.
(5) Shafaati, M.; Saidijam, M.; Soleimani, M.; Hazrati, F.; Mirzaei, R.; Amirheidari, B.; Tanzadehpanah, H.; Karampoor, S.; Kazemi, S.; Yavari, B.; Mahaki, H.; Safaei, M.; Rahbarizadeh, F.; Samadi, P.; Ahmadyousefi, Y. A Brief Review on DNA Vaccines in the Era of COVID-19. *Future Virol.* **2022**, *17*, 49.
(6) Hogan, M. J.; Pardi, N. MRNA Vaccines in the COVID-19 Pandemic and Beyond. *Ann. Rev. Med.* **2022**, *73*, 17.
(7) Kheirvari, M.; Liu, H.; Tumban, E. Virus-like Particle Vaccines and Platforms for Vaccine Development. *Viruses* **2023**, *15*, 1109.
(8) Roldão, A.; Mellado, M. C. M.; Castilho, L. R.; Carrondo, M. J. T.; Alves, P. M. Virus-like Particles in Vaccine Development. *Expert Rev. Vaccines* **2010**, *9*, 1149.
(9) de Pinho Favaro, M. T.; Atienza-Garriga, J.; Martínez-Torró, C.; Parladé, E.; Vázquez, E.; Corchero, J. L.; Ferrer-Miralles, N.; Villaverde, A. Recombinant Vaccines in 2022: A Perspective from the Cell Factory. *Microb. Cell Fact.* **2022**, *21* (1), 203.
(10) Tariq, H.; Batool, S.; Asif, S.; Ali, M.; Abbasi, B. H. Virus-Like Particles: Revolutionary Platforms for Developing Vaccines Against Emerging Infectious Diseases. *Front. Microbiol.* **2022**, DOI: 10.3389/fmicb.2021.790121.
(11) Berzofsky, J. A.; Ahlers, J. D.; Belyakov, I. M. Strategies for Designing and Optimizing New Generation Vaccines. *Nature Rev. Immunol.* **2001**, *1*, 209.
(12) Moyle, P. M.; Toth, I. Modern Subunit Vaccines: Development, Components, and Research Opportunities. *ChemMedChem.* **2013**, *8* (3), 360.
(13) Doytchinova, I. A.; Flower, D. R. VaxiJen: A Server for Prediction of Protective Antigens, Tumour Antigens and Subunit Vaccines. *BMC Bioinform.* **2007**, *8*, DOI: 10.1186/1471-2105-8-4.
(14) Bobbala, S.; Hook, S. Is There an Optimal Formulation and Delivery Strategy for Subunit Vaccines? *Pharm. Res.* **2016**, *33*, 2078.
(15) Sánchez, J. M.; López-Laguna, H.; Álamo, P.; Serna, N.; Sánchez-Chardi, A.; Nolan, V.; Cano-Garrido, O.; Casanova, I.; Unzueta, U.; Vazquez, E.; Mangues, R.; Villaverde, A. Artificial Inclusion Bodies for Clinical Development. *Adv. Sci.* **2020**, *7* (3), DOI: 10.1002/advs.201902420.
(16) Parladé, E.; Sánchez, J. M.; López-Laguna, H.; Unzueta, U.; Villaverde, A.; Vázquez, E. Protein Features Instruct the Secretion Dynamics from Metal-Supported Synthetic Amyloids. *Int. J. Biol. Macromol.* **2023**, *250*, 126164.
(17) López-Laguna, H.; Sánchez, J.; Unzueta, U.; Mangues, R.; Vázquez, E.; Villaverde, A. Divalent Cations: A Molecular Glue for Protein Materials. *Trends Biochem. Sci.* **2020**, *45* (11), 992.
(18) López-Laguna, H.; Rueda, A.; Martínez-Torró, C.; Sánchez-Alba, L.; Carratalá, J. V.; Atienza-Garriga, J.; Parladé, E.; Sánchez, J. M.; Serna, N.; Voltà-Durán, E.; Ferrer-Miralles, N.; Reverter, D.; Mangues, R.; Villaverde, A.; Vázquez, E.; Unzueta, U. Biofabrication of Self-Assembling Covalent Protein Nanoparticles through Histidine-Templated Cysteine Coupling. *ACS Sustain Chem. Eng.* **2023**, *11* (10), 4133.
(19) Álamo, P.; Parladé, E.; Favaro, M. T. P.; Gallardo, A.; Mendoza, R.; Ferreira, L. C. S.; Roher, N.; Mangues, R.; Villaverde, A.; Vázquez, E. Probing the Biosafety of Implantable Artificial Secretory Granules for the Sustained Release of Bioactive Proteins. *ACS Appl. Mater. Interfaces* **2023**, *15* (33), 39167−39175.
(20) Soragni, A.; Maji, S. K.; Riek, R. Toward a Comprehension of Functional Aggregation into Amyloids in Pituitary Secretory Granules. *Amyloid* **2010**, *17*, 41.
(21) Jacob, R. S.; Anoop, A.; Maji, S. K. Protein Nanofibrils as Storage Forms of Peptide Drugs and Hormones. *Adv. Exp. Med. Biol.* **2019**, *1174*, 265−290.
(22) Jacob, R. S.; Das, S.; Ghosh, S.; Anoop, A.; Jha, N. N.; Khan, T.; Singru, P.; Kumar, A.; Maji, S. K. Amyloid Formation of Growth Hormone in Presence of Zinc: Relevance to Its Storage in Secretory Granules. *Sci. Rep.* **2016**, *6* (1), 1−18.
(23) Maji, S. K.; Perrin, M. H.; Sawaya, M. R.; Jessberger, S.; Vadodaria, K.; Rissman, R. A.; Singru, P. S.; Nilsson, K. P. R.; Simon, R.; Schubert, D.; Eisenberg, D.; Rivier, J.; Sawchenko, P.; Vale, W.; Riek, R. Functional Amyloids as Natural Storage of Peptide Hormones in Pituitary Secretory Granules. *Science* **2009**, *325* (5938), 328−332.
(24) Chatterjee, D.; Jacob, R. S.; Ray, S.; Navalkar, A.; Singh, N.; Sengupta, S.; Gadhe, L.; Kadu, P.; Datta, D.; Paul, A.; Arunima, S.; Mehra, S.; Pindi, C.; Kumar, S.; Singru, P. S.; Senapati, S.; Maji, S. K. Co-Aggregation and Secondary Nucleation in the Life Cycle of Human Prolactin/Galanin Functional Amyloids. *Elife* **2022**, *11*, DOI: 10.7554/eLife.73835.
(25) Álamo, P.; Parladé, E.; López-Laguna, H.; Voltà-Durán, E.; Unzueta, U.; Vazquez, E.; Mangues, R.; Villaverde, A. Ion-Dependent Slow Protein Release from in Vivo Disintegrating Micro-Granules. *Drug Delivery* **2021**, *28* (1), 2383−2391.
(26) Serna, N.; Falgàs, A.; García-León, A.; Unzueta, U.; Núñez, Y.; Sánchez-Chardi, A.; Martínez-Torró, C.; Mangues, R.; Vazquez, E.; Casanova, I.; Villaverde, A. Time-Prolonged Release of Tumor-Targeted Protein-MMAE Nanoconjugates from Implantable Hybrid Materials. *Pharmaceutics* **2022**, *14* (1), 192.
(27) Corchero, J. L.; Favaro, M. T. P.; Márquez-Martínez, M.; Lascorz, J.; Martínez-Torró, C.; Sánchez, J. M.; López-Laguna, H.; de Souza Ferreira, L. C.; Vázquez, E.; Ferrer-Miralles, N.; Villaverde, A.; Parladé, E. Recombinant Proteins for Assembling as Nano- and Micro-Scale Materials for Drug Delivery: A Host Comparative Overview. *Pharmaceutics* **2023**, *15* (4), 1197.
(28) López-Laguna, H.; Sánchez, J. M.; Carratalá, J. V.; Rojas-Peña, M.; Sánchez-García, L.; Parladé, E.; Sánchez-Chardi, A.; Voltà-Durán, E.; Serna, N.; Cano-Garrido, O.; Flores, S.; Ferrer-Miralles, N.; Nolan, V.; de Marco, A.; Roher, N.; Unzueta, U.; Vazquez, E.; Villaverde, A. Biofabrication of Functional Protein Nanoparticles through Simple His-Tag Engineering. *ACS Sustain. Chem. Eng.* **2021**, *9* (36), 12341.
(29) Pulendran, B.; Arunachalam, P. S.; O'Hagan, D. T. Emerging Concepts in the Science of Vaccine Adjuvants. *Nat. Rev. Drug Discovery* **2021**, *20* (6), 454−475.
(30) Hoffman, W. P.; Ness, D. K.; van Lier, R. B. L. Analysis of Rodent Growth Data in Toxicology Studies. *Toxicol. Sci.* **2002**, *66* (2), 313−319.
(31) Quast, I.; Tarlinton, D. Time Is of the Essence for Vaccine Success. *Nat. Immunol.* **2022**, *23* (11), 1517−1519.
(32) Chen, T. Y.; Cheng, W. J.; Horng, J. C.; Hsu, H. Y. Artificial Peptide-Controlled Protein Release of Zn^{2+}-Triggered, Self-Assembled Histidine-Tagged Protein Microparticle. *Colloids Surf. B Biointerfaces* **2020**, *187*, 110644.
(33) López-Laguna, H.; Voltà-Durán, E.; Parladé, E.; Villaverde, A.; Vázquez, E.; Unzueta, U. Insights on the Emerging Biotechnology of Histidine-Rich Peptides. *Biotechnol. Adv.* **2022**, *54*, 107817.
(34) Blanco, L. P.; Evans, M. L.; Smith, D. R.; Badtke, M. P.; Chapman, M. R. Diversity, Biogenesis and Function of Microbial Amyloids. *Trends Microbiol.* **2012**, *20*, 66.
(35) Levkovich, S. A.; Gazit, E.; Laor Bar-Yosef, D. Two Decades of Studying Functional Amyloids in Microorganisms. *Trends Microbiol.* **2021**, *29*, 251.
(36) Sergeeva, A. V.; Galkin, A. P. Functional Amyloids of Eukaryotes: Criteria, Classification, and Biological Significance. *Curr. Genetics* **2020**, *66*, 849.
(37) Balistreri, A.; Goetzler, E.; Chapman, M. Functional Amyloids Are the Rule Rather than the Exception in Cellular Biology. *Microorganisms* **2020**, *8* (12), 1951.
(38) Sánchez, J. M.; Carratalá, J. V.; Serna, N.; Unzueta, U.; Nolan, V.; Sánchez-Chardi, A.; Voltà-Durán, E.; López-Laguna, H.; Ferrer-Miralles, N.; Villaverde, A.; Vazquez, E. The Poly-Histidine Tag H6Mediates Structural and Functional Properties of Disintegrating, Protein-Releasing Inclusion Bodies. *Pharmaceutics* **2022**, *14* (3), 602.

(39) Lacroix, E.; Pereira, L.; Yoo, B.; Coyle, K. M.; Chandhok, S.; Zapf, R.; Marijan, D.; Morin, R. D.; Vlachos, S.; Harden, N.; Audas, T. E. Evolutionary conservation of systemic and reversible amyloid aggregation. *J Cell Sci* **2021**, *134* (22), jcs258907.
(40) Poothong, J.; Pottekat, A.; Siirin, M.; Campos, A. R.; Paton, A. W.; Paton, J. C.; Lagunas-Acosta, J.; Chen, Z.; Swift, M.; Volkmann, N.; Hanein, D.; Yong, J.; Kaufman, R. J. Factor VIII exhibits chaperone-dependent and glucose-regulated reversible amyloid formation in the endoplasmic reticulum. *Blood* **2020**, *135* (21), 1899−1911.
(41) McGlinchey, R. P.; Lee, J. C. Reversing the Amyloid Trend: Mechanism of Fibril Assembly and Dissolution of the Repeat Domain from a Human Functional Amyloid. *Isr. J. Chem.* **2017**, *57*, 613.
(42) Cao, Y.; Adamcik, J.; Diener, M.; Kumita, J. R.; Mezzenga, R. Different Folding States from the Same Protein Sequence Determine Reversible vs Irreversible Amyloid Fate. *J. Am. Chem. Soc.* **2021**, *143* (30), 11473−11481.
(43) Buchanan, J. A.; Varghese, N. R.; Johnston, C. L.; Sunde, M. Functional Amyloids: Where Supramolecular Amyloid Assembly Controls Biological Activity or Generates New Functionality. *Journal of Molecular Biology* **2023**, *435* (11), 167919.
(44) Hymer, W. C.; Kraemer, W. J. Resistance exercise stress: theoretical mechanisms for growth hormone processing and release from the anterior pituitary somatotroph. *J Appl Physiol* **2023**, *123*, 1867−1878.
(45) Omar-Hmeadi, M.; Idevall-Hagren, O. Insulin granule biogenesis and exocytosis. *Cell. Mol. Life Sci.* **2021**, *78*, 1957−1970.
(46) Serna, N.; López-Laguna, H.; Aceituno, P.; Rojas-Peña, M.; Parladé, E.; Voltà-Durán, E.; Martinez-Torró, C.; Sánchez, J. M.; Di Somma, A.; Carratalá, J. V.; et al. Efficient Delivery of Antimicrobial Peptides in an Innovative, Slow-Release Pharmacological Formulation. *Pharmaceutics* **2023**, *15*, 2632.
(47) Céspedes, M. V.; Cano-Garrido, O.; Álamo, P.; Sala, R.; Gallardo, A.; Serna, N.; Falgàs, A.; Voltà-Durán, E.; Casanova, I.; Sánchez-Chardi, A.; López-Laguna, H.; Sánchez-García, L.; Sánchez, J. M.; Unzueta, U.; Vázquez, E.; Mangues, R.; Villaverde, A. Engineering Secretory Amyloids for Remote and Highly Selective Destruction of Metastatic Foci. *Adv. Mater.* **2020**, *32*, 1907348.
(48) Serna, N.; Cano-Garrido, O.; Sánchez, J. M.; Sánchez-Chardi, A.; Sánchez-García, L.; López-Laguna, H.; Fernández, E.; Vázquez, E.; Villaverde, A. Release of functional fibroblast growth factor-2 from artificial inclusion bodies. *J Control Release* **2020**, *327*, 61−69.
(49) Sanchez, J. M.; López-Laguna, H.; Serna, N.; Unzueta, U.; Clop, P. D.; Villaverde, A.; Vazquez, E. Engineering the Performance of Artificial Inclusion Bodies Built of Catalytic β-Galactosidase. *ACS Sustain. Chem. Eng.* **2021**, *9* (6), 2552.
(50) Schneider, C. G.; Taylor, J. A.; Sibilo, M. Q.; Miura, K.; Mallory, K. L.; Mann, C.; Karch, C.; Beck, Z.; Matyas, G. R.; Long, C. A.; et al. Orientation of Antigen Display on Self-Assembling Protein Nanoparticles Influences Immunogenicity. *Vaccines* **2021**, *9* (2), 103.
(51) Murin, C. D.; Wilson, I. A.; Ward, A. B. Antibody Responses to Viral Infections: A Structural Perspective across Three Different Enveloped Viruses. *Nat. Microbiol.* **2019**, *4*, 734.
(52) Rink, L.; Gabriel, P. Zinc and the Immune System. In *Proceedings of the Nutrition Society*, Vol. *59*; 2000; p 541,.
(53) Ko, M. K.; Kim, H. W.; Park, S. H.; Park, J. H.; Kim, S. M.; Lee, M. J. The Role of Zinc Sulfate in Enhancing Cellular and Humoral Immune Responses to Foot-and-Mouth Disease Vaccine. *Virus Res.* **2023**, *335*, 199189.
(54) Prem, K.; Choi, Y. H.; Bénard, É.; Burger, E. A.; Hadley, L.; Laprise, J.-F.; Regan, C.; Drolet, M.; Sy, S.; Abbas, K.; Kim, J. J.; Brisson, M.; Jit, M. Global Impact and Cost-Effectiveness of One-Dose Versus Two-Dose Human Papillomavirus Vaccination Schedules: A Comparative Modelling Analysis. *SSRN Electron. J.* **2021**, DOI: 10.2139/ssrn.3779876.
(55) Brotherton, J. M.; Budd, A.; Rompotis, C.; Bartlett, N.; Malloy, M. J.; Andersen, R. L.; Coulter, K. A.; Couvee, P. W.; Steel, N.; Ward, G. H.; Saville, M. Is One Dose of Human Papillomavirus Vaccine as Effective as Three?: A National Cohort Analysis. *Papillomavirus Res.* **2019**, *8*, 100177.
(56) Markowitz, L. E.; Drolet, M.; Perez, N.; Jit, M.; Brisson, M. Human Papillomavirus Vaccine Effectiveness by Number of Doses: Systematic Review of Data from National Immunization Programs. *Vaccine* **2018**, *36* (32), 4806.
(57) Kreimer, A. R.; Herrero, R.; Sampson, J. N.; Porras, C.; Lowy, D. R.; Schiller, J. T.; Schiffman, M.; Rodriguez, A. C.; Chanock, S.; Jimenez, S.; Schussler, J.; Gail, M. H.; Safaeian, M.; Kemp, T. J.; Cortes, B.; Pinto, L. A.; Hildesheim, A.; Gonzalez, P. Evidence for Single-Dose Protection by the Bivalent HPV Vaccine—Review of the Costa Rica HPV Vaccine Trial and Future Research Studies. *Vaccine* **2018**, *36* (32), 4774.
(58) Zhu, J.; Jain, S.; Sha, J.; Batra, H.; Ananthaswamy, N.; Kilgore, P. B.; Hendrix, E. K.; Hosakote, Y. M.; Wu, X.; Olano, J. P.; Kayode, A.; Galindo, C. L.; Banga, S.; Drelich, A.; Tat, V.; Tseng, C. T. K.; Chopra, A. K.; Rao, V. B. A Bacteriophage-Based, Highly Efficacious, Needle- and Adjuvant-Free, Mucosal COVID-19 Vaccine. *mBio* **2022**, *13* (4), DOI: 10.1128/mbio.01822-22.
(59) Song, S. J.; Shin, G. I.; Noh, J.; Lee, J.; Kim, D. H.; Ryu, G.; Ahn, G.; Jeon, H.; Diao, H. P.; Park, Y.; Kim, M. G.; Kim, W. Y.; Kim, Y. J.; Sohn, E. J.; Song, C. S.; Hwang, I. Plant-Based, Adjuvant-Free, Potent Multivalent Vaccines for Avian Influenza Virus via Lactococcus Surface Display. *J. Integr. Plant Biol.* **2021**, *63* (8), 1505.
(60) Ribeiro, A. C. M.; Guedes, L. K. N.; Moraes, J. C. B.; Saad, C. G. S.; Aikawa, N. E.; Calich, A. L.; França, I. L. A.; Carvalho, J. F.; Sampaio-Barros, P. D.; Goncalves, C. R.; Borba, E. F.; Timenetsky, M. D. C. S.; Precioso, A. R.; Duarte, A.; Bonfa, E.; Laurindo, I. M. M. Reduced Seroprotection after Pandemic H1N1 Influenza Adjuvant-Free Vaccination in Patients with Rheumatoid Arthritis: Implications for Clinical Practice. *Ann. Rheum. Dis.* **2011**, *70* (12), 2144.
(61) López-Laguna, H.; Parladé, E.; Álamo, P.; Sánchez, J. M.; Voltà-Durán, E.; Serna, N.; Sánchez-García, L.; Cano-Garrido, O.; Sánchez-Chardi, A.; Villaverde, A. In Vitro Fabrication of Microscale Secretory Granules. *Adv. Funct. Mater.* **2021**, *31*, 2100914.